

Field-responsive ion transport in nanopores

Weiyi Lu,¹ Aijie Han,² Taewan Kim,³ Venkata K. Punyamurtula,² Xi Chen,⁴ and Yu Qiao^{1,3,a)}

¹Department of Structural Engineering, University of California-San Diego, La Jolla, California 92093-0085, USA

²Department of Chemistry, University of Texas-Pan America, Edinburg, Texas 78539, USA

³Program of Materials Science and Engineering, University of California-San Diego, La Jolla, California 92093, USA

⁴Department of Civil Engineering and Engineering Mechanics, Columbia University, New York, New York 10027, USA

(Received 7 October 2008; accepted 20 December 2008; published online 13 January 2009)

The transport behavior of solvated ions in nanopores of a zeolite Y is field responsive. As an external electric field is applied, the observed change in effective solid-liquid interfacial tension is contradictory to the prediction of classic electrochemistry theory; it considerably increases no matter whether the applied voltage is positive or negative. This may be attributed to the breakdown of solvated ion and double-layer structures in the nanoenvironment. © 2009 American Institute of Physics. [DOI: 10.1063/1.3070531]

The study on ion transport in confining nanoenvironment has been active for a couple of decades, driven by the development of biomedicine, catalysis, energy-related applications, etc.^{1–3} In a nanochannel, especially when the characteristic length scale is comparable with the Debye length, the solvated structures of ions would be influenced by the channel wall.^{4,5} The distribution of water molecules can be highly distorted along the axial direction, which would be energetically unfavorable in a bulk phase.^{6–10} As most of ions are exposed to the nanochannel wall, the amount of ions in the interior is much smaller than that at a large solid surface. As a result, the mass and energy exchange between the interface zone and the bulk phase is significantly suppressed.^{11–13} The equilibrium conditions at the Gouy–Chapman and Stern layers and their dependence on environmental factors can be affected by the far field.^{14–17} The time constants of surface adsorption/desorption may increase.^{18,19} Moreover, anions may directly interact the solid atoms, causing a “squeezing” effect.²⁰

As ions are adsorbed by a solid surface, countercharges can be induced in the solid phase, leading to the formation of electrostatics.²¹ This phenomenon has been observed in nanoporous electrodes under various conditions.^{22–25} If a low voltage is applied, additional oppositely charged ions would be adsorbed; that is, the equilibrium surface ion density is dependent on the external electric field.²⁶ While this concept has been studied intensively by a number of research groups, e.g., Ref. 27, the influence of applied electric field on ion transport behaviors is still relatively uninvestigated, imposing tremendous challenges to the research on multiphase sensing, programmable catalysis, controllable chromatography, etc. Previous studies in this area were focused on computer simulations.²⁸ Experimental results that can validate and/or provide system parameters for the simulations are scarce.

One difficulty in the experimental study on field responsiveness of ion transport in nanochannels is the lack of direct measurement method of system free energy. As ions trans-

port in a nanochannel, at the steady state the system free energy would be different from that of the initial state. In a test where spontaneous ion diffusion is dominant, such information would be lost. The recently developed pressure-induced infiltration (PII) technique provides a promising way to solve this problem.^{29–31} In a PII test, the nanochannel surfaces must be hydrophobic, so that under ambient condition the nanochannels are empty. The liquid phase enters the nanochannels only when a sufficiently high external pressure P is applied.

In the current study, we investigated a zeolite Y (ZY) obtained from the Zeolyst. The as-received material was in powder form, with the particle size of about 10 μm and the silica-to-alumina ratio of 80. According to a gas absorption analysis by using a Micrometrics ASAP-2000 Analyzer, the nanopore size was 0.7 nm, the specific surface area was 710 m^2/g , and the porosity was 220 mm^3/g . The x-ray diffraction analysis result showed that the material was well crystallized. About 2 g of the ZY sample was dried in vacuum at 120 $^\circ\text{C}$ for 6 h and then sealed in a vertical furnace with a cylindrical quartz reactor. At 400 $^\circ\text{C}$, a slow nitrogen flow carrying silicon tetrachloride⁴ vapor was maintained across the reactor for 2 h. The ZY sample was filtered, repeatedly rinsed by acetone, methanol, and warm water until the pH value reached 7. The material was combusted in air at 600 $^\circ\text{C}$ for 1.5 h, and finally rinsed in warm water and dried in vacuum at 120 $^\circ\text{C}$ for 12 h.

The treated ZY sample was hydrophobic. As it was immersed in an aqueous solution, it could not be soaked up spontaneously. The behavior of the noncharged system has been described elsewhere.³² In order to produce a charged system, the electrical conductivity of the nanoporous phase must be improved, for which two parts of Dendritic-3 μ copper powders were uniformly mixed with one part of ZY. The copper particle size was 3 μm , fitting well into the gaps among the zeolite crystals. The ZY-Cu mixture was placed in a steel cylinder and compressed at 20 MPa for 5 min by a type 5580 Instron machine, forming a dense disk. Each disk contained 0.2 g of ZY crystals and had a diameter of 19 mm. Figure 1 depicts the experimental setup of the charged samples. A ZY-Cu disk was placed on a platinum counter-

^{a)}Author to whom correspondence should be addressed. Electronic mail: yqiao@ucsd.edu.

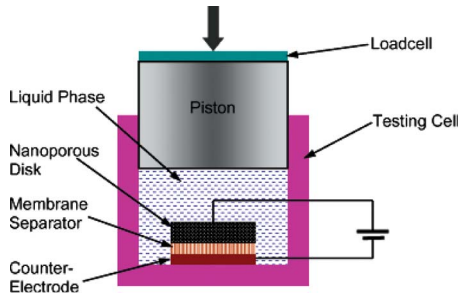


FIG. 1. (Color online) Schematic of the charged experimental setup.

electrode, separated by a 30 μm thick Celgard-3501 membrane. The electrodes were immersed in a saturated lithium chloride solution (819 g/l) in a stainless steel cylinder, sealed by a stainless steel piston. The cross-sectional area of the piston was $A_p=286 \text{ mm}^2$. Two silver wires were extended from the electrode and the counterelectrode, respectively, through which an external voltage was applied by a Proteck 6030 dc power supply. The piston was driven into the testing cell at a constant rate of 1 mm/min by the Instron machine. When the pressure reached 85 MPa, the piston was moved out of the testing cell at the same speed. Typical sorption isotherm curves are shown in Fig. 2. During the loading process, the applied voltage was maintained at either 500 or -500 mV .

At the beginning stage, the quasihydrostatic pressure in the liquid phase P is relatively low, which cannot overcome the capillary effect of the nanopores. With a large pressure increase, the system volume variation is relatively small. When P reaches the critical value, the increase in effective interfacial tension can be balanced by the release of pressure, and thus the pressure-induced infiltration takes place. Around this pressure range, the system volume decreases rapidly, causing the formation of an infiltration plateau in the sorption isotherm curve. In the current study, for self-comparison purpose, the critical infiltration pressure P_{in} is taken as the pressure at the middle point of the infiltration plateau. Eventually, when the nanopores are filled, the infiltration plateau ends and the sorption isotherm curve converges back to the low-compressibility profile. The unloading path is different from the loading path probably due to the influences of entrapped vapor molecules,^{14,30} the energy barriers among tetrahedral sites along nanopore surfaces,³³ and the heat exchange between the confined liquid and the environment,³⁴ the details of which are still under investigation.

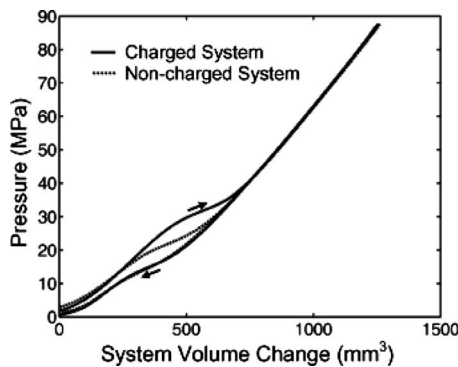


FIG. 2. Typical sorption isotherm curves. The arrows show that the system volume decreases when an external pressure is applied and increases when the pressure is reduced.

The testing data show that the values of P_{in} of the charged system and the noncharge system are considerably different. The P_{in} of the noncharged system is 23 MPa, and that of the systems charged at 500 and -500 mV are 33 and 33.2 MPa, respectively. Within the tolerance of the current testing setup, no significant difference can be detected. Clearly, the dominant factor of P_{in} variation is the magnitude of the external electric field, not its direction. Note that the critical pressure of nanopore collapse is at the level of a few hundreds megapascals.³⁵ In the pressure range of the current study the nanoporous structure is quite stable.

The change in interfacial tension with external field has long been known as the electrowetting effect.³⁶ When a liquid phase and a solid phase contact each other. The surface ions induce countercharges in the solid phase, causing a zeta potential ϕ . At a constant temperature, the zeta potential can be related to the interfacial tension γ through the Lippmann equation $\partial\gamma/\partial\phi=-\sigma$, where $\sigma=\int C_e \times d\phi$ is the surface ion density and C_e is the interface capacity. As a first-order approximation, C_e may be simplified as a material constant and the interfacial tension can be calculated by the classic Helmholtz–Perrin equation³⁷

$$\gamma = \gamma_0 - \frac{\varepsilon\varepsilon_0}{2d} \phi^2, \quad (1)$$

where γ_0 is a reference interfacial tension, ε is the dielectric constant, ε_0 is the permittivity of free space, and d is the characteristic length of the interface double layer. As an external electric field is applied, the zeta potential is changed and the interfacial tension varies. If the solid and the liquid phases are in direct contact, usually the applied voltage should be below the thresholds of surface chemical reactions. In this voltage range, the variation in ϕ can be 20%–30%, depending on the ion properties and concentration.³⁸ It can be seen that no matter whether ϕ is positive or negative, the interfacial tension always decreases with the increase in the applied voltage, since the induced charges in the solid phase would always attract oppositely charged ions. The distribution of ions tends to be in the most energetically favorable configuration, and therefore the system free energy is lowered.

The testing data in Fig. 2 indicate that as a 500 mV voltage is applied, the infiltration pressure changes significantly. As the liquid phase enters the nanopores, the system free energy varies by $\gamma \times A$, where $A \approx 2\pi r d_i$ is the area of the nanopore surface exposed to the liquid phase, r is the nanopore radius, and d_i is the effective infiltration depth. The released mechanical energy in the bulk liquid phase can be estimated as $P_{\text{in}} \times V$, where $V \approx \pi r^2 d_i$ is the infiltration volume. At the equilibrium condition, $\gamma = P_{\text{in}} r / 2$. For the non-charged system, γ is about 3.4 mJ/m²; for the charged system, γ is nearly 4.9 mJ/m², higher than the former by about 50%. The magnitude of the interfacial tension variation is larger than but close to the prediction of the classic theory. It is insensitive to the direction of the external electric field, which fits with Eq. (1). The electrode in Fig. 1 may be regarded as zeolite crystals embedded in a semicontinuous copper matrix. As the external voltage is applied on the copper matrix, it induces surface charges at the nanopore surfaces, which affects the zeta potential.

A remarkable phenomenon is that as the external electric field is applied the value of the effective interfacial tension

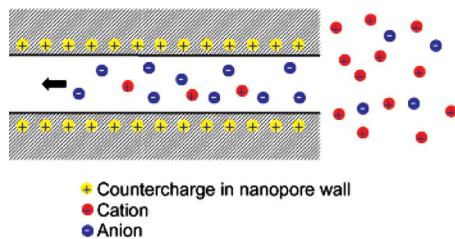


FIG. 3. (Color online) Schematic of ion transport in a charged nanopore. Solvent molecules are not shown.

increases. This observation cannot be explained by the classic theory discussed above, since at a large solid surface the rearrangement of the ions should reduce the system free energy. It may be related to the confinement effect of the nanopore walls, as depicted in Fig. 3. In a nanopore, the induced charges in nanopore walls would attract oppositely charged ions in the liquid phase and repel like-charged ones. Different from a solid electrode, in the nanoenvironment there is no space for the bulk phase. Since the nanopore size is comparable with the ion size, by taking into account the van der Waals distance, across the cross section there would be only one or a few ions, all of which are directly exposed to the solid atoms. The thermal disarrays that usually exist immediately next to the interface double layer are left outside the nanoporous crystals, far away from the confined liquid. Consequently, a confined monopolar liquid phase can be formed. To separate the confined ions from the bulk phase, additional work must be done and thus the system free energy tends to increase.

The amount of the additional work done on the charged system can be estimated from Fig. 2 as the area in between the infiltration plateaus of the charged and noncharged systems, which is around 2 J/g, or 2.8 mJ/m². If the intrinsic interfacial tension decrease caused by the applied voltage is 20% (i.e., 0.7 mJ/m²), the additional work associated with the charge separation in nanopores should be $\Delta U_s = 2.2$ mJ/m². If the nanopore radius is taken as 0.3 nm, the system free energy change can be calculated as $\Delta U = 2\Delta U_s/r = 14.7$ mJ/mm³. As a first-order approximation, the amount of the separated charge may be assessed as $Q = \Delta U/C = 3.6 \times 10^{-9}$ C/mm³ or 2.2×10^{10} e/mm³, where $C \approx \epsilon_e \epsilon_0 / 2D$ is the effective system capacity per unit area, $\epsilon = 40$ is the dielectric constant of the liquid phase, $D = 5$ μ m is the average radius of ZY crystals, and “e” indicates electron charge. It can be seen that Q is around one-billionth of the ion density of saturated lithium chloride solution (1.2×10^{19} e/mm³).

Because of the small nanopore size of the zeolite, the confined ions cannot be fully solvated by water molecules, and thus both cations and anions may be in direct contact with the solid atoms. Since the ion charges of lithium cation and chlorine anion are the same and the solid nanopore surface is quite neutral,³⁹ as the direction of the external electric field is shifted the ion behaviors in nanopores would not be significantly affected, which explains why the value of system free energy change is only dependent on the magnitude of the applied voltage.

In summary, it is observed in experiment that the characteristics of field responsiveness of ion transport in nanopores are fundamentally different from that at a large solid surface. The effective interfacial tension increases significantly as an external electric field is applied, which can be

attributed to the charge separation associated with the formation of a monopolar confined liquid phase.

This study was supported by the National Science Foundation and The Sandia National Laboratory under Grant No. CMS-0623973.

- ¹A. Noy, H. G. Park, F. Fornasiero, J. K. Holt, C. P. Grigoropoulos, and O. Bakajin, *Nanotoday* **2**, 22 (2007).
- ²X. J. Gong, J. Y. Li, H. J. Lu, R. Z. Wan, J. C. Li, J. Hu, and H. P. Fang, *Nat. Nanotechnol.* **2**, 709 (2007).
- ³H. T. Liu and G. Y. Zhu, *J. Power Sources* **171**, 1054 (2007).
- ⁴S. Joseph, R. J. Mashl, E. Jakobsson, and N. R. Aluru, *Nano Lett.* **3**, 1399 (2003).
- ⁵S. M. Cory, Y. Y. Liu, and M. I. Glavinovic, *Biochim. Biophys. Acta* **1768**, 2319 (2007).
- ⁶T. Sumikama, S. Saito, and I. Ohmine, *J. Phys. Chem. B* **110**, 20671 (2006).
- ⁷L. L. Huang, Q. Shao, L. H. Lu, X. H. Lu, L. Z. Zhang, J. Wang, and S. Y. Jiang, *Phys. Chem. Chem. Phys.* **8**, 3836 (2006).
- ⁸R. W. Murray, *Chem. Rev.* **108**, 2688 (2008).
- ⁹D. Y. Lu, A. Aksimentiev, A. Y. Shih, E. Cruz-Chu, P. L. Freddolino, and K. Schulten, *Phys. Biol.* **3**, S40 (2006).
- ¹⁰Y. H. Zhang, B. Zhang, and H. S. White, *J. Phys. Chem. B* **110**, 1768 (2006).
- ¹¹G. X. Cao, Y. Qiao, Q. L. Zhou, and X. Chen, *Philos. Mag. Lett.* **88**, 371 (2008).
- ¹²M. H. Weng, W. J. Lee, S. P. Ju, C. H. Chao, N. K. Hsieh, J. G. Chang, and H. L. Chen, *J. Chem. Phys.* **128**, 174705 (2008).
- ¹³L. Liu, Y. Qiao, and X. Chen, *Appl. Phys. Lett.* **92**, 101927 (2008).
- ¹⁴Y. Qiao, G. Cao, and X. Chen, *J. Am. Chem. Soc.* **129**, 2355 (2007).
- ¹⁵W. K. Liu, E. G. Karpov, S. Zhang, and H. S. Park, *Comput. Methods Appl. Mech. Eng.* **193**, 1529 (2004).
- ¹⁶A. Han, X. Chen, and Y. Qiao, *Langmuir* **24**, 7044 (2008).
- ¹⁷A. Han and Y. Qiao, *Langmuir* **23**, 11396 (2007).
- ¹⁸Y. Qiao, A. Han, and V. K. Punyamurtula, *J. Phys. D* **41**, 085505 (2008).
- ¹⁹Y. Qiao, V. K. Punyamurtula, and A. Han, *Appl. Phys. Lett.* **91**, 153102 (2007).
- ²⁰A. Tanimura, A. Kovalenko, and F. Hirata, *Langmuir* **23**, 1507 (2007).
- ²¹E. M. McCash, *Surface Chemistry* (Oxford University Press, New York, 2001).
- ²²J. Yang, F. Z. Lu, L. W. Kostiuk, and D. Y. Kwok, *J. Nanosci. Nanotechnol.* **5**, 648 (2005).
- ²³F. H. J. van der Heyden, D. Stein, K. Besteman, S. G. Lemay, and C. Dekker, *Phys. Rev. Lett.* **96**, 224502 (2006).
- ²⁴Y. Qiao, V. K. Punyamurtula, and A. Han, *J. Power Sources* **164**, 931 (2007).
- ²⁵Y. Qiao, V. K. Punyamurtula, and A. Han, *J. Power Sources* **183**, 403 (2008).
- ²⁶J. O. Bockris and S. U. M. Khan, *Surface Electrochemistry* (Springer, New York, 1993).
- ²⁷A. K. Shukla, S. Sampath, and K. Vijayamohan, *Curr. Sci.* **79**, 1656 (2000).
- ²⁸L. Zeng, G. H. Zuo, X. J. Gong, H. J. Lu, C. L. Wang, K. F. Wu, and R. Z. Wan, *Chin. Phys. Lett.* **25**, 1486 (2008).
- ²⁹A. Han and Y. Qiao, *J. Am. Chem. Soc.* **128**, 10348 (2006).
- ³⁰A. Han, X. Kong, and Y. Qiao, *J. Appl. Phys.* **100**, 014308 (2006).
- ³¹X. Kong and Y. Qiao, *Philos. Mag. Lett.* **85**, 331 (2005).
- ³²A. Han and Y. Qiao, *Appl. Phys. Lett.* **91**, 173123 (2007).
- ³³X. Chen, G. Cao, A. Han, V. K. Punyamurtula, L. Liu, P. J. Culligan, T. Kim, and Y. Qiao, *Nano Lett.* **8**, 2988 (2008).
- ³⁴Y. Qiao, V. K. Punyamurtula, G. Xian, V. M. Karbhari, and A. Han, *Appl. Phys. Lett.* **92**, 063109 (2008).
- ³⁵A. Han, V. K. Punyamurtula, W. Lu, and Y. Qiao, *J. Appl. Phys.* **103**, 084318 (2008).
- ³⁶V. S. Bagotsky, *Fundamentals of Electrochemistry* (Wiley, New York, 2005).
- ³⁷A. W. Adamson and A. P. Gast, *Physical Chemistry of Surfaces* (Wiley, New York, 1997).
- ³⁸C. H. Hamann, A. Jammatt, and W. Vielstich, *Electrochemistry* (Wiley, New York, 1998).
- ³⁹J. C. Jansen, M. Stocker, J. Weitkamp, and H. G. Karge, *Advanced Zeolite Science and Applications* (Elsevier, New York, 1994).